

Geophysical Research Letters

RESEARCH LETTER

10.1029/2018GL081080

Key Points:

- Circulation changes have offset most western U.S. snowpack loss from global warming since the 1980s
- Circulation changes are likely a result of natural variability, not anthropogenic forcing
- Snowpack loss will likely accelerate in coming decades as the phase of natural variability subsides

Supporting Information:

- Supporting Information S1

Correspondence to:

N. Siler,
nick.siler@oregonstate.edu

Citation:

Siler, N., Proistosescu, C., & Po-Chedley, S. (2019). Natural variability has slowed the decline in western U.S. snowpack since the 1980s. *Geophysical Research Letters*, 46, 346–355. <https://doi.org/10.1029/2018GL081080>

Received 25 OCT 2018

Accepted 7 DEC 2018

Accepted article online 17 DEC 2018

Published online 11 JAN 2019

Natural Variability Has Slowed the Decline in Western U.S. Snowpack Since the 1980s

Nicholas Siler¹ , Cristian Proistosescu² , and Stephen Po-Chedley³ 

¹ College of Earth, Ocean, and Atmospheric Sciences, Oregon State University, Corvallis, OR, USA, ² Joint Institute for the Study of the Atmosphere and the Ocean, University of Washington, Seattle, WA, USA, ³ Program for Climate Model Diagnosis and Intercomparison, Lawrence Livermore National Laboratory, Livermore, CA, USA

Abstract Spring snowpack in the mountains of the western United States has not declined substantially since the 1980s, despite significant global and regional warming. Here we show that this apparent insensitivity of snowpack to warming is a result of changes in the atmospheric circulation over the western United States, which have reduced snowpack losses due to warming. Climate model simulations indicate that the observed circulation changes have been driven in part by a shift in Pacific sea surface temperatures that is attributable to natural variability, and not part of the simulated response to anthropogenic forcing. Removing the influence of natural variability reveals a robust anthropogenic decline in western U.S. snowpack since the 1980s, particularly during the early months of the accumulation season (October–November). These results suggest that the recent stability of western U.S. snowpack will be followed by a period of accelerated decline once the current mode of natural variability subsides.

Plain Language Summary Melting snowpack is a vital source of water in the western United States during the summer, when rainfall is usually scarce. Although the amount of water contained in the snowpack has declined over the past century, it has been surprisingly stable since the 1980s, despite 1 °C of warming over the same period. At first glance, this result might appear to indicate that the snowpack is quite resilient to warming. However, here we show that the contribution of global warming to western U.S. snowpack loss has in reality been large and widespread since the 1980s, but mostly offset by natural variability in the climate system. This result points to a faster rate of snowpack loss in coming decades, when the impact of global warming is more likely to be amplified, rather than offset, by natural variability.

1. Introduction

Snowpack in the western United States acts as a natural reservoir, storing water during the cool wet season (October–March) and releasing it to the landscape during the warm dry season (Barnett et al., 2005; Cayan, 1996). Containing more than 150 cubic kilometers of water at its peak—usually reached around 1 April—the western U.S. winter snowpack holds about as much water as all the man-made reservoirs in the western United States combined (Mote et al., 2018). Since 1950, the snowpack on 1 April has decreased by 15–30% over much of the western United States, as warmer temperatures have caused a shift from snow to rain, particularly at low elevations (Mote et al., 2018). Models indicate a further decrease in winter snowpack of perhaps 60% by 2050 (Ashfaq et al., 2013; Fyfe et al., 2017), leading to a dramatic reduction in summer stream flows in a region where water shortages are already common (Barnett et al., 2005; Christensen et al., 2004).

Despite this alarming forecast, snowpack has been surprisingly stable in recent decades. Figure 1a shows the trends in 1-April snowpack at 329 automated Snowfall Telemetry (SNOTEL) stations where the average 1-April snowpack contains at least 25 cm of water equivalent. Trends were calculated over 35 winters beginning in 1983–1984, when the network reached nearly its current level of coverage (Figure S1 in the supporting information), and 1 year after the record-setting El Niño of 1982–1983. During this 35-year period, only four sites experienced a statistically significant decline in 1-April snowpack (95% confidence), while 208 sites (63%) experienced an insignificant decline. The other 117 sites (36%) experienced a positive (but statistically insignificant) trend. We find a similar result when we repeat the analysis using regionally averaged time series of 1-April snowpack (Figure 1b), with no region exhibiting a statistically significant trend since 1983–1984. This result is consistent with Mudryk et al. (2018), who found similar stability in the spring snowpack of

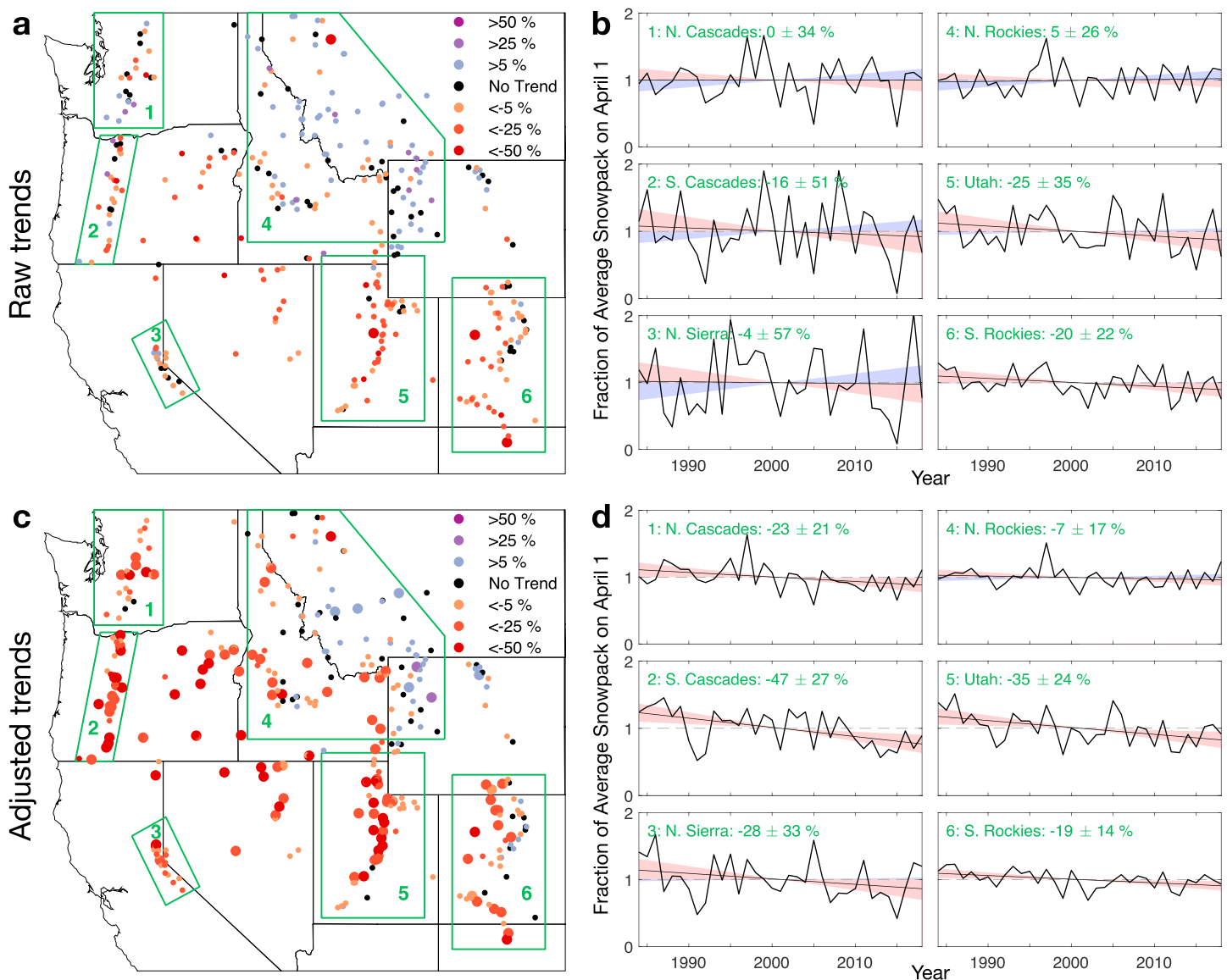


Figure 1. Raw and dynamically adjusted trends in 1-April snowpack (as measured by snow water equivalent) at 329 Snowfall Telemetry sites across the western United States between 1984 and 2018 (water years). (a) Raw trends. Large circles are statistically significant ($p = 0.05$). (b) Regionally averaged time series and trend estimates for six regions outlined in (a): 1: northern Cascades; 2: southern Cascades; 3: northern Sierra Nevada; 4: northern Rocky Mountains; 5: Utah; 6: southern Rocky Mountains. Shaded cones represent the 95% confidence range of the trend estimate, with red indicating a negative trend, and blue indicating a positive trend. (c, d) As in (a) and (b) but after dynamical adjustment. All values are expressed as a fraction of the 35-year average 1-April snowpack.

western Canada over roughly the same time period. Meanwhile, the average winter surface temperature over the western U.S. increased by more than 1°C during this period—on par with the average warming trend across global land surfaces (Figure S2). Taken at face value, this result suggests that winter snowpack in the western United States may be remarkably insensitive to warming, seemingly contradicting model forecasts of rapid decline (Ashfaq et al., 2013; Fyfe et al., 2017).

On decadal timescales, however, snowpack is influenced not only by anthropogenic warming, but also by natural variability in the large-scale atmospheric circulation (Deser et al., 2012). Depending on its phase, natural variability can either offset or accelerate the changes in snowpack due to anthropogenic warming (Cayan, 1996; McCabe & Wolock, 2009; Mote, 2006; Smoliak et al., 2010; Stoelinga et al., 2010). In order to quantify the anthropogenic trend in western U.S. snowpack, one must first remove the component of the trend that can be attributed to natural variability in the atmosphere.

One approach that previous studies have taken to minimize the noise of natural variability has been to focus on the ratio of snowpack to accumulated precipitation (S/P), which tends to be more sensitive than snowpack to changes in temperature (Barnett et al., 2008; Pierce et al., 2008; Pierce & Cayan, 2013). Across the SNOTEL network, we similarly find more robust declines in S/P than in snowpack alone (Figure S3 vs. Figures 1a and 1b). However, while S/P may exhibit a clearer warming signal, it provides little insight into the magnitude of snowpack change resulting from anthropogenic warming versus natural variability.

In this paper, we use a method called “dynamical adjustment” to quantify the influences of both anthropogenic warming and natural variability on 1-April snowpack at each of the 329 SNOTEL stations shown in Figure 1a. We find that, since 1983–1984, changes in the atmospheric circulation have contributed to a $\sim 30\%$ increase in 1-April snowpack in the Cascade Mountains and northern Sierra Nevada, and an increase of $\sim 10\%$ in Utah and the Northern Rocky Mountains, offsetting much of the decline due to global warming. Simulations performed with an atmospheric general circulation model (AGCM) and prescribed historical sea surface temperatures (SSTs) indicate that the observed circulation change has likely been driven in part by internal atmospheric variability, and in part by a shift in Pacific SSTs toward the cool phase of the Interdecadal Pacific Oscillation (IPO). We find that such SST/circulation trends are not part of the simulated response to anthropogenic forcing in coupled GCMs but are likely associated with low-frequency natural variability that will eventually subside, ushering in a period of accelerated snowpack loss.

2. Data and Methods

2.1. Dynamical Adjustment

While there are various ways to perform dynamical adjustment (Deser et al., 2016; Fereday et al., 2018; Lehner et al., 2018, 2017; Merrifield et al., 2017; O'Reilly et al., 2017), here we use the well-known method of partial least squares regression (Christian et al., 2016; Deser et al., 2014; Smoliak et al., 2015, 2010; Wallace et al., 2012). At each SNOTEL station, we adjust the 35-year time series of net snowpack accumulation (i.e., the “predictand”) during three separate stages of the accumulation season: early (October–November), middle (December–January), and late (February–March). Net accumulation during each stage was computed from daily observations of snow water equivalent supplied by the Natural Resources Conservation Service. As predictors, we use three variables from MERRA-2 reanalysis (Gelaro et al., 2017) that are representative of the large-scale atmospheric circulation: (1) pressure at mean sea level, and geopotential height at (2) 500 hPa and (3) 250 hPa. We remove the global means of (2) and (3) to account for global warming. We restrict the domain of each predictor field to the Northern Hemisphere south of 60°N , and to the Pacific/North America sector between 110°E and 290°E . However, our results are essentially unchanged when the domain is expanded to the full Northern Hemisphere (not shown).

To begin, we apply a 15-year high-pass filter to both the predictand and predictors and compute the correlation matrix \mathbf{X} between the predictand and predictors at each grid point. Filtering avoids fitting to the anthropogenic trend, and/or to low-frequency variability that could impact the trend on decadal timescales. We then project the observed predictor anomalies onto \mathbf{X} , producing a time series \mathbf{y} . The relationship between \mathbf{X} and \mathbf{y} is directly analogous to the relationship between an empirical orthogonal function and its corresponding principal component (Siler et al., 2018). Finally, we regress \mathbf{y} out of both the predictand and predictors and repeat the entire procedure two more times to yield the dynamically adjusted snowpack accumulation. The adjusted 1-April snowpack is found by adding the adjusted subseasonal accumulations. While the full set of predictor patterns is unwieldy, Figure S4 gives an example of the average predictor patterns among SNOTEL stations in the southern Cascades of Oregon—a region where changes in the atmospheric circulation have had a particularly large influence on recent snowpack trends, as discussed in section 3.

To minimize overfitting, we use leave-p-out cross validation, so that each year's adjustment is based on the correlation matrix from all other years. To evaluate the success of this approach, we have tested the same algorithm on thousands of sets of 10 randomly generated subseasonal time series, designed to approximate the ~ 10 degrees of freedom in western U.S. snowpack. Using the same subseasonal predictor fields described above, we find that dynamical adjustment reduces the average season-total variance by $5.1 \pm 5.5\%$ (1σ). By comparison, the average variance in 1-April snowpack across all SNOTEL stations decreases by 47.2% after dynamical adjustment. This demonstrates that the large majority of snowpack variance removed through dynamical adjustment is physically related to variability in the atmospheric circulation, and not a result of overfitting.

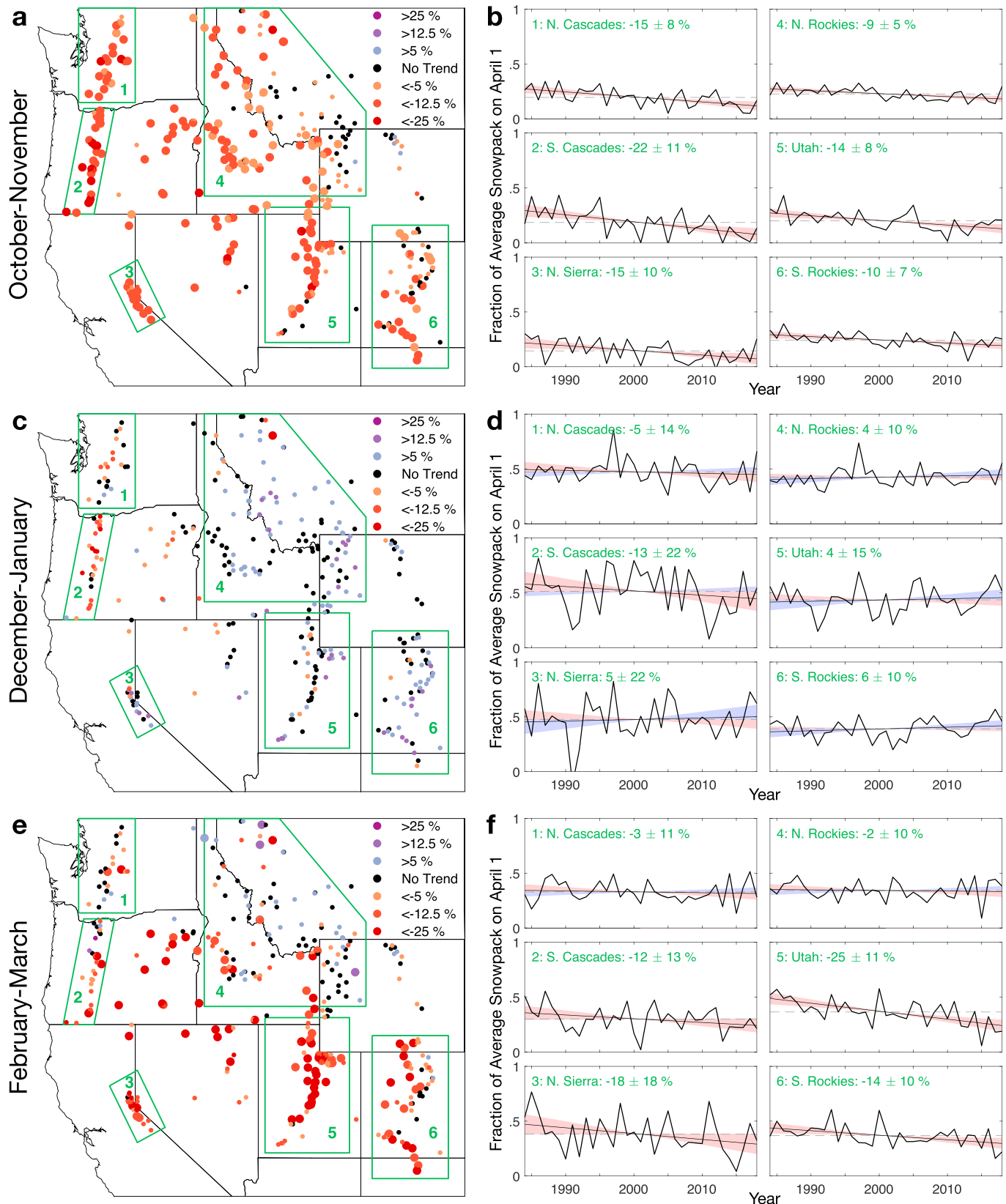


Figure 2. Dynamically-adjusted trends in snowpack accumulation during the early (October–November; a and b), middle (December–January; c and d), and late (February–March; e and f) stages of the accumulation season. Like in Figure 1, all values are expressed as a fraction of the 35-year average of 1-April snowpack.

2.2. Trend Significance

Snowpack trends are calculated using linear least squares regression. To determine trend significance (both raw and adjusted), we first compute the p value of the trend in each time series as if it were a single hypothesis test, accounting for year-to-year persistence (Wilks, 2011). Then, to account for multiple hypotheses, we apply the false-discovery-rate test to this set of p values, choosing a two-tailed confidence level of 95% ($\alpha = 0.05$), and adjusting for fewer degrees of freedom due to strong spatial correlations (Wilks, 2016).

2.3. Other Observations

Gridded SST observations are taken from version 2 of the monthly NOAA Optimal Interpolation SST data set (OISSTv2; Reynolds et al., 2002). Global-mean and regional-mean surface warming is estimated from the gridded Goddard Institute for Space Studies Surface Temperature analysis (Hansen et al., 2010).

2.4. Model Simulations

Prescribed SST simulations are provided by NOAA's Facility for Climate Assessments. We analyze 30 simulations performed with the ECHAM5 AGCM at $0.75^\circ \times 0.75^\circ$ resolution with prescribed historical SSTs (Roeckner et al., 2003). As of October, 2018, ECHAM5 was the only GCM with a large ensemble of prescribed-SST simulations spanning the entire 35-year analysis period. Coupled GCM simulations were performed as part of the latest Coupled Model Intercomparison Project (CMIP5; Taylor et al., 2012). We have included all available models and ensemble members in our analysis. Trends were calculated for each ensemble member from 1983–1984 to 2017–2018 by concatenating output from historical (through 2005) and RCP8.5 (after 2005) experiments, which best approximate historical emissions (Hayhoe et al., 2017).

3. Results

Figure 1c shows the trends in 1-April snowpack between 1983–1984 and 2017–2018 after dynamically adjusting the net subseasonal accumulation. In contrast to the raw time series (Figure 1a), which exhibit almost no significant changes since 1984, the trends in the dynamically adjusted time series are significantly negative at 106 sites (32%), and significantly positive at just 7 sites (2%), all in northwestern Wyoming or southwestern Montana. When applied to the regionally averaged time series, dynamical adjustment reveals significant declines in every region except the northern Sierra Nevada and the northern Rocky Mountains, where the trends are negative but not statistically significant (Figure 1d).

Comparing the three stages of the accumulation season (Figure 2), we find that the most robust changes have occurred early in the season, when 199 sites (60%) show a significant decline (Figures 2a and 2b). Early-season declines are largest on the West Coast and in Utah, where above-freezing mean temperatures leave the snowpack particularly vulnerable to warming (Figure S5a). Late season declines are less widespread (Figures 2e and 2f), but still significant at 94 sites (29%), including most of Utah and the southern Rockies (regions 5 and 6). In contrast, midseason snowpack is less sensitive to warming (Figures 2c and 2d), likely because the average temperature in December and January has remained below freezing at most sites (Figure S5b; Kapnick & Hall, 2012).

The increased statistical significance of the dynamically-adjusted trends compared to the raw trends can be explained in part by the smaller variance of the adjusted time series after the circulation-driven variability is removed. But the effect of dynamical adjustment goes beyond a simple reduction in variance; it also includes substantial changes in the trends themselves. In the southern Cascades of Oregon (region 2), for example, the raw time series exhibits a decrease in 1-April snowpack of $16 \pm 51\%$, while the adjusted time series exhibits a much larger decrease of $47 \pm 27\%$ (all percentage changes are relative to the 1984–2018 mean 1-April snowpack, while uncertainty estimates indicate 95% confidence). The difference—an increase of 31%—represents the change in snowpack due to changes in the atmospheric circulation. Similarly positive contributions to snowpack trends from the atmospheric circulation are found over most of the western United States, with every region except the southern Rocky Mountains exhibiting adjusted trends that are at least 10% more negative than the raw trends in the same region. These differences imply that, in the absence of changes in the atmospheric circulation, the decline in western U.S. snowpack since the 1980s would have been substantially larger than has been observed.

To better understand the influence of the atmospheric circulation on western U.S. snowpack trends, we show the dynamical contribution to snowpack trends at each SNOTEL site (Figure 3a) alongside the trends in the winter-mean circulation over the same time period (Figure 3b). The dynamical contribution in Figure 3a is

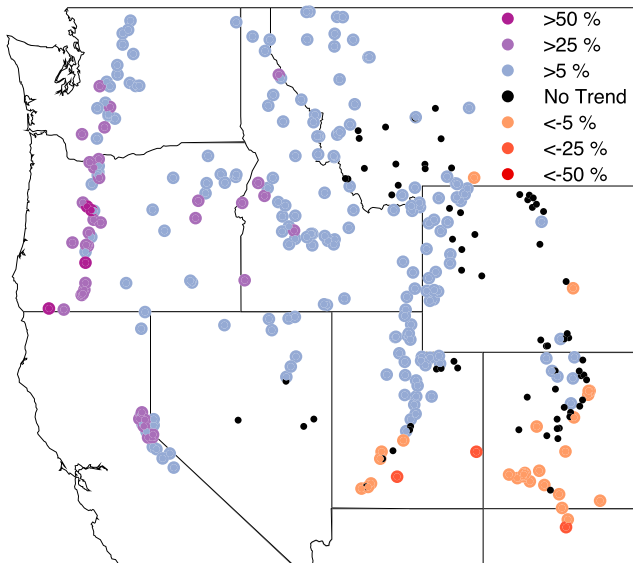
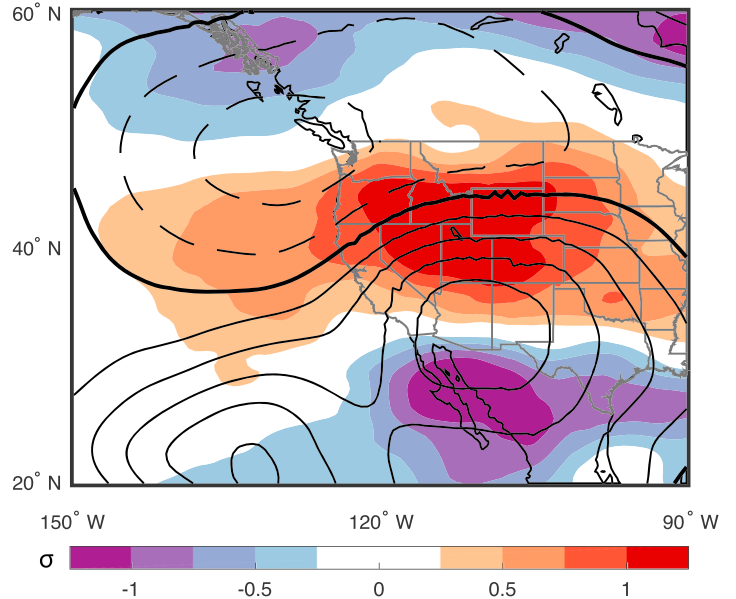
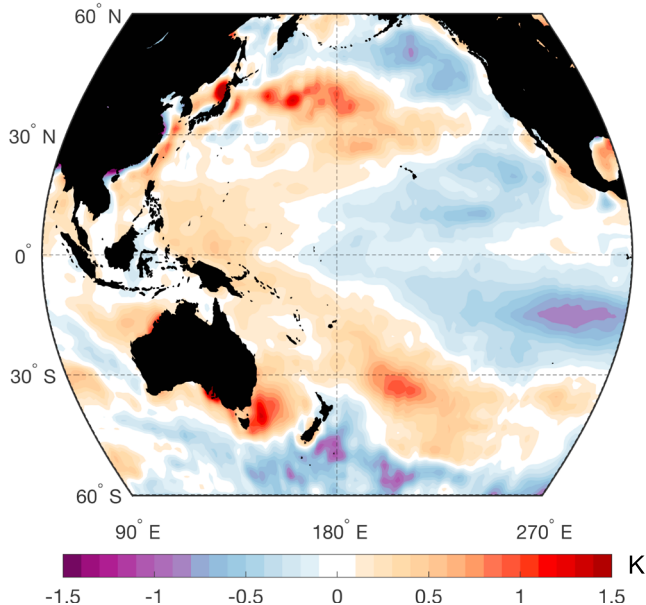
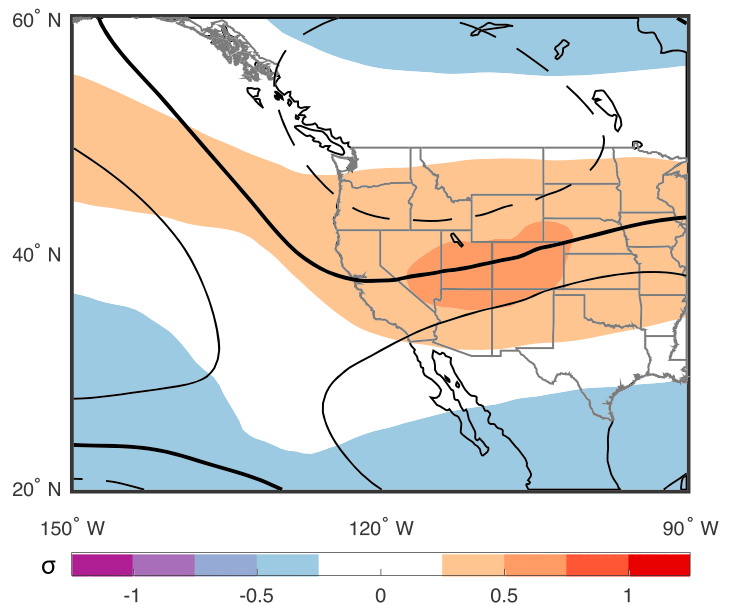
a Snowpack trend due to circulation**b** Circulation trend: Observed**c** SST* trend: Observed**d** Circulation trend: AGCM ens. mean

Figure 3. (a) The dynamical contribution to 1-April snowpack trends between 1984 and 2018, equivalent to the difference between the raw and adjusted trends in Figures 1a and 1c. (b) The observed trend in winter-mean U_{500} (colors) and Z_{500} (contours), normalized by the interannual standard deviation (σ) at each grid point. The Z_{500} trend was computed after subtracting the global-mean value in each winter. (c) The observed trend in winter-mean SST*, defined as the local SST minus the average SST within the region shown. (d) As in (b) but for the ensemble mean of 30 simulations from the ECHAM5 atmospheric GCM run with prescribed historical SSTs. SST = sea surface temperature; AGCM = atmospheric general circulation model.

equal to the difference between the raw and adjusted snowpack trends in Figures 1a and 1c. It averages 13% across all SNOTEL sites but is substantially larger in the Cascades and Sierra Nevada (regions 1–3), where it averages 29%. These dynamically induced snowpack trends have coincided with enhanced zonal winds at 500 hPa (U_{500} ; Figure 3b, colors), driven by a steepening of the north-south gradient in geopotential height (Z_{500}) over the western United States (Figure 3b, black contours). Stronger U_{500} is associated with greater moisture transport to the West Coast, and with larger orographic enhancement of precipitation at high elevations (Luce et al., 2013; Siler et al., 2013), consistent with the positive dynamical contribution to snowpack trends in Figure 3a.

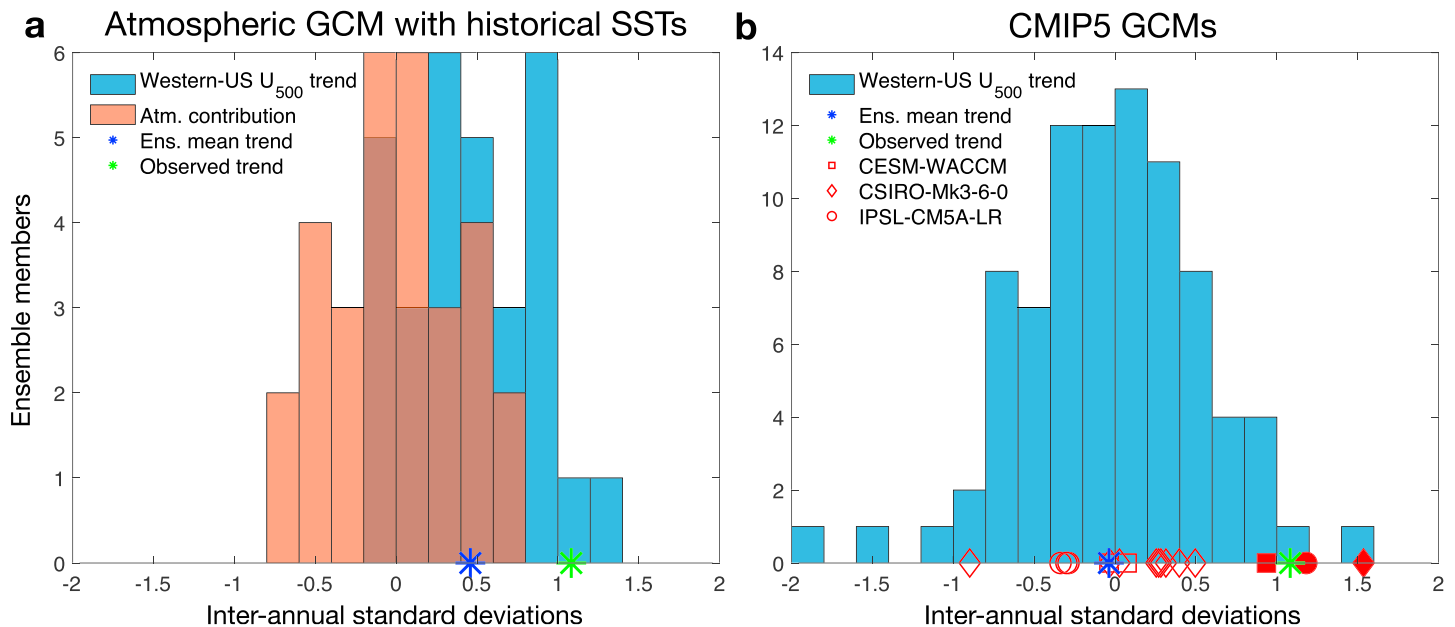


Figure 4. (a) The distribution of trends in winter-mean U_{500} over the western United States between 1983–1984 and 2017–2018, normalized by the detrended interannual standard deviation, within a 30-member ensemble of simulations from the ECHAM5 atmospheric GCM run with prescribed historical SSTs. Blue represents the full distribution, while orange represents the atmospheric (i.e., non-SST-driven) component of the distribution, as measured by the departure of each ensemble member from the ensemble-mean trend (blue star). The observed trend (green star) falls within the full distribution, but outside the atmospheric component of the distribution, indicating that SST changes likely account for some of the observed trend. (b) As in (a) but for an 86-member ensemble of coupled GCM simulations from CMIP5. Solid red shapes show the three largest U_{500} trends among all ensemble members, which were simulated by the following models: CESM-WACCM (square), CSIRO-Mk3-6-0 (diamond), and IPSL-CM5A-LR (circle). Hollow red shapes show the trends across all other simulations performed by the same GCMs. SST = sea surface temperature; CMIP5 = Coupled Model Intercomparison Project phase 5; GCM = general circulation model.

The observed circulation trends are likely driven in part by changes in the spatial pattern of global SSTs (Figure 3c). In particular, suppressed warming in the eastern tropical Pacific and enhanced warming in the northwestern and southwestern Pacific are consistent with a shift toward the cool phase of the IPO (Power et al., 1999) between 1983–1984 and 2017–2018 (Figure S6a)—a phenomenon which has previously been linked to the recent global warming “hiatus” (Dai et al., 2015). In addition to its global cooling effect, the negative IPO phase is also associated with enhanced U_{500} over the western U.S., consistent with observed trends (Figure S6b).

To further evaluate the contribution of SSTs to observed circulation trends, we turn to an ensemble of 30 simulations from the ECHAM5 AGCM performed using prescribed historical SSTs and radiative forcing. Because the simulations are identical except for small perturbations in their initial conditions, the ensemble mean captures the component of atmospheric variability within the simulations that is driven by changes in SSTs and atmospheric composition, while the ensemble spread reflects the influence of internal atmospheric variability. Compared with the observed circulation trends, the ensemble-mean trends have similar spatial structure (Figure 3d), but their magnitude is only about half as large over the western United States, implying that SSTs alone do not account for all of the observed circulation trends. On the other hand, observed circulation trends are also not explained by internal atmospheric variability alone, as indicated by the relatively small ensemble spread in U_{500} trends over the western United States (Figure 4a). Given that observed U_{500} trends fall well within the simulated range (Figure 4a), these results indicate that SSTs and internal atmospheric variability have both contributed to—and together explain—the dynamical suppression of snowpack decline since the 1980s.

4. Future Implications

Looking forward, the implications of our results depend on whether the observed SST/circulation changes in recent decades have been part of the climate’s response to anthropogenic forcing, or simply a result of low-frequency natural variability. To answer this question, we compare the observed SST/circulation trends in Figures 3b and 3c with those simulated by a large ensemble ($n = 86$) of coupled oceanic-atmospheric

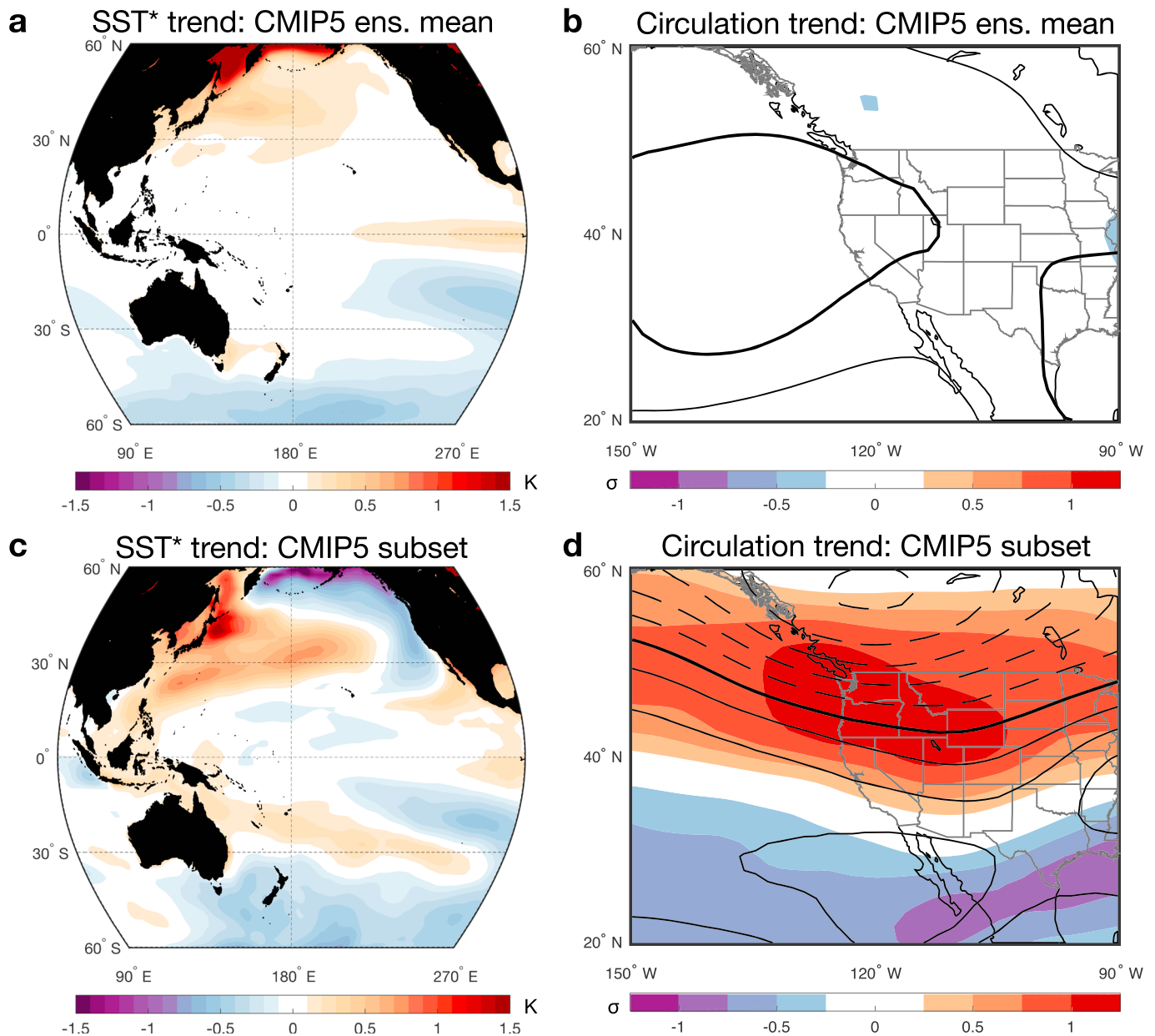


Figure 5. (a) The ensemble-mean trend in winter-mean (October–March) SST* in CMIP5 simulations run with historical and projected radiative forcing between 1983–1984 and 2017–2018. (b) The ensemble-mean trend in normalized winter-mean U_{500} (colors) and Z_{500} (contours). The Z_{500} trend was computed after subtracting the global-mean value in each winter. (c) As in (a) but for a subset of three ensemble members (CESM-WACCM, CSIRO-Mk3-6-0, and IPSL-CM5A-LR) that exhibited trends in U_{500} over the western United States that were similar to the observed trend. (d) As in (b) but for the same subset of simulations included in (c). SST = sea surface temperature; CMIP5 = Coupled Model Intercomparison Project phase 5; GCM = general circulation model.

GCMs from CMIP5 (Taylor et al., 2012) over the same 35-year time period (Figure 5; Table S1). In contrast to the observed trends, the ensemble mean of these simulations shows little evidence of an IPO-like shift in SST patterns (Figure 5a), or of a substantial change in the atmospheric circulation over the western United States (Figure 5b), suggesting that observed trends are not primarily driven by anthropogenic forcing.

On the other hand, the observed trend in U_{500} over the western United States does fall within the range that one would expect from natural variability, based on the CMIP5 ensemble spread (Figure 4b). Furthermore, among the ensemble members that exhibit the largest U_{500} trends over the western United States (Figure 5d), SST trends resemble the observed shift toward the cool phase of the IPO (Figure 5c), supporting our hypothesis that circulation trends have been driven in part by shifting SST patterns. Meanwhile, the same subset of

GCMs produced a wide range of U_{500} trends in other identical simulations (Figure 4b, red shapes), confirming that the CMIP5 ensemble spread is primarily a reflection of natural variability, and not of differences in model physics.

Of course, it is possible that observed SST/circulation trends represent a component of the forced response that most GCMs do not capture (Kohyama & Hartmann, 2017). If so, then changes in the atmospheric circulation may continue to offset some of the decline in western U.S. snowpack due to warming. But if recent circulation changes have instead been a result of natural variability—the more likely outcome in our view, given the close correspondence between observed SST changes and the IPO—then the relative stability of western U.S. snowpack since the 1980s is unlikely to persist, portending an accelerated decline in coming decades as the phase of variability becomes less favorable for snowpack accumulation.

Acknowledgments

C. P. was supported by a postdoctoral fellowship from the University of Washington Joint Institute for the Study of the Atmosphere and the Ocean. The work of S. P. was performed under the auspices of the U.S. Department of Energy (DOE) by LLNL under Contract DE-AC52-07NA27344 with support provided by the LLNL-LDRD Program under Project 18-ERD-054. Model output and observations can be accessed at the following websites. Snow water equivalent and temperature data at each SNOTEL station: <https://www.wcc.nrcs.usda.gov/snow/>. Gridded SST data: <https://www.esrl.noaa.gov/psd/data/gridded/data.noaa.oisst.v2.html>. MERRA-2 reanalysis: <https://gmao.gsfc.nasa.gov/reanalysis/MERRA-2/>. GISTEMP gridded surface temperature analysis: <https://www.esrl.noaa.gov/psd/ECHAM5/prescribed-SST/simulations/>. CMIP5 simulations: <https://esgf-node.llnl.gov/search/cmip5/>.

References

- Ashfaq, M., Ghosh, S., Kao, S.-C., Bowling, L. C., Mote, P., Touma, D., et al. (2013). Near-term acceleration of hydroclimatic change in the western U.S. *Journal of Geophysical Research: Atmospheres*, 118, 10,676–10,693. <https://doi.org/10.1002/jgrd.50816>
- Barnett, T. P., Adam, J. C., & Lettenmaier, D. P. (2005). Potential impacts of a warming climate on water availability in snow-dominated regions. *Nature*, 438(7066), 303–309.
- Barnett, T. P., Pierce, D. W., Hidalgo, H. G., Bonfils, C., Santer, B. D., Das, T., et al. (2008). Human-induced changes in the hydrology of the western United States. *Science*, 319(5866), 1080–1083.
- Cayan, D. R. (1996). Interannual climate variability and snowpack in the western United States. *Journal Climate*, 9(5), 928–948.
- Christensen, N. S., Wood, A. W., Voisin, N., Lettenmaier, D. P., & Palmer, R. N. (2004). The effects of climate change on the hydrology and water resources of the Colorado River basin. *Climatic Change*, 62(1-3), 337–363.
- Christian, J. E., Siler, N., Koutnik, M., & Roe, G. (2016). Identifying dynamically induced variability in glacier mass-balance records. *Journal of Climate*, 29(24), 8915–8929.
- Dai, A., Fyfe, J. C., Xie, S.-P., & Dai, X. (2015). Decadal modulation of global surface temperature by internal climate variability. *Nature Climate Change*, 5(6), 555–559.
- Deser, C., Phillips, A. S., Alexander, M. A., & Smoliak, B. V. (2014). Projecting North American climate over the next 50 years: Uncertainty due to internal variability. *Journal Climate*, 27(6), 2271–2296.
- Deser, C., Phillips, A., Bourdette, V., & Teng, H. (2012). Uncertainty in climate change projections: The role of internal variability. *Climate Dynamics*, 38(3-4), 527–546.
- Deser, C., Terray, L., & Phillips, A. S. (2016). Forced and internal components of winter air temperature trends over North America during the past 50 years: Mechanisms and implications. *Journal Climate*, 29(6), 2237–2258.
- Fereday, D., Chadwick, R., Knight, J., & Scaife, A. A. (2018). Atmospheric dynamics is the largest source of uncertainty in future winter European rainfall. *Journal Climate*, 31(3), 963–977.
- Fyfe, J. C., Derksen, C., Mudryk, L., Flato, G. M., Santer, B. D., Swart, N. C., et al. (2017). Large near-term projected snowpack loss over the western United States. *Nature Communications*, 8, 14996.
- Gelaro, R., McCarty, W., Suárez, M. J., Todling, R., Molod, A., Takacs, L., et al. (2017). The modern-era retrospective analysis for research and applications, version 2 (MERRA-2). *Journal Climate*, 30(14), 5419–5454.
- Hansen, J., Ruedy, R., Sato, M., & Lo, K. (2010). Global surface temperature change. *Reviews of Geophysics*, 48, RG4004. <https://doi.org/10.1029/2010RG000345>
- Hayhoe, K., Edmonds, J., Koppp, R. E., LeGrande, A. N., Sanderson, B. M., Wehner, M. F., & Wuebbles, D. J. (2017). Climate models, scenarios, and projections. In D. J. Wuebbles et al. (Eds.), *Climate Science Special Report: Fourth National Climate Assessment* (Vol. i, pp. 133–160). Washington, DC: U.S. Global Change Research Program.
- Kapnick, S., & Hall, A. (2012). Causes of recent changes in western North American snowpack. *Climate Dynamics*, 38(9-10), 1885–1899.
- Kohyama, T., & Hartmann, D. L. (2017). Nonlinear ENSO warming suppression (NEWS). *Journal Climate*, 30(11), 4227–4251.
- Lehner, F., Deser, C., Simpson, I. R., & Terray, L. (2018). Attributing the U.S. Southwest's recent shift into drier conditions. *Geophysical Research Letters*, 45, 6251–6261. <https://doi.org/10.1029/2018GL078312>
- Lehner, F., Deser, C., & Terray, L. (2017). Toward a new estimate of “time of emergence” of anthropogenic warming: Insights from dynamical adjustment and a large initial-condition model ensemble. *Journal Climate*, 30(19), 7739–7756.
- Luce, C. H., Abatzoglou, J. T., & Holden, Z. A. (2013). The missing mountain water: Slower westerlies decrease orographic enhancement in the Pacific Northwest USA. *Science*, 342(6164), 1360–1364.
- McCabe, G. J., & Wolock, D. M. (2009). Recent declines in western U.S. snowpack in the context of twentieth-century climate variability. *Earth Interactions*, 13(12), 1–15.
- Merrifield, A., Lehner, F., Xie, S.-P., & Deser, C. (2017). Removing circulation effects to assess central U.S. land-atmosphere interactions in the CESM Large Ensemble. *Geophysical Research Letters*, 44, 9938–9946. <https://doi.org/10.1002/2017GL074831>
- Mote, P. W. (2006). Climate-driven variability and trends in mountain snowpack in western North America. *Journal Climate*, 19(23), 6209–6220.
- Mote, P. W., Li, S., Lettenmaier, D. P., Xiao, M., & Engel, R. (2018). Dramatic declines in snowpack in the western U.S. *Climate and Atmospheric Science*, 1(1), 2.
- Mudryk, L. R., Derksen, C., Howell, S., Laliberté, F., Thackeray, C., Sospedra-Alfonso, R., et al. (2018). Canadian snow and sea ice: Historical trends and projections. *The Cryosphere*, 12, 1157–1176.
- O'Reilly, C. H., Woollings, T., & Zanna, L. (2017). The dynamical influence of the Atlantic Multidecadal Oscillation on continental climate. *Journal Climate*, 30(18), 7213–7230.
- Pierce, D. W., Barnett, T. P., Hidalgo, H. G., Das, T., Bonfils, C., Santer, B. D., et al. (2008). Attribution of declining Western U.S. snowpack to human effects. *Journal Climate*, 21(23), 6425–6444.
- Pierce, D. W., & Cayan, D. R. (2013). The uneven response of different snow measures to human-induced climate warming. *Journal Climate*, 26(12), 4148–4167.
- Power, S., Casey, T., Folland, C., Colman, A., & Mehta, V. (1999). Inter-decadal modulation of the impact of ENSO on Australia. *Climate Dynamics*, 15(5), 319–324.

- Reynolds, R. W., Rayner, N. A., Smith, T. M., Stokes, D. C., & Wang, W. (2002). An improved in situ and satellite SST analysis for climate. *Journal Climate*, 15(13), 1609–1625.
- Roeckner, E., Bäuml, G., Bonaventura, L., Brokopf, R., Esch, M., Giorgetta, M., et al. (2003). The atmospheric general circulation model ECHAM5. Part I: Model description. Max Planck Institute for Meteorology.
- Siler, N., Po-Chedley, S., & Bretherton, C. S. (2018). Variability in modeled cloud feedback tied to differences in the climatological spatial pattern of clouds. *Climate Dynamics*, 50(3-4), 1209–1220.
- Siler, N., Roe, G., & Durran, D. (2013). On the dynamical causes of variability in the rain-shadow effect: A case study of the Washington Cascades. *Journal of Hydrometeorology*, 14(1), 122–139.
- Smoliak, B. V., Wallace, J. M., Lin, P., & Fu, Q. (2015). Dynamical adjustment of the Northern Hemisphere surface air temperature field: Methodology and application to observations. *Journal Climate*, 28(4), 1613–1629.
- Smoliak, B. V., Wallace, J. M., Stoelinga, M. T., & Mitchell, T. P. (2010). Application of partial least squares regression to the diagnosis of year-to-year variations in Pacific Northwest snowpack and Atlantic hurricanes. *Geophysical Research Letters*, 37, L03801. <https://doi.org/10.1029/2009GL041478>
- Stoelinga, M. T., Albright, M. D., & Mass, C. F. (2010). A new look at snowpack trends in the Cascade Mountains. *Journal Climate*, 23(10), 2473–2491.
- Taylor, K. E., Stouffer, R. J., & Meehl, G. A. (2012). An overview of CMIP5 and the experiment design. *Bulletin of the American Meteorological Society*, 93(4), 485–498.
- Wallace, J. M., Fu, Q., Smoliak, B. V., Lin, P., & Johanson, C. M. (2012). Simulated versus observed patterns of warming over the extratropical northern hemisphere continents during the cold season. *Proceedings of the National Academy of Sciences of the United States of America*, 109(36), 14337–14342.
- Wilks, D. S. (2011). *Statistical methods in the atmospheric sciences*. Cambridge, MA: Elsevier/Academic Press.
- Wilks, D. S. (2016). "The stippling shows statistically significant grid points": How research results are routinely overstated and overinterpreted, and what to do about it. *Bulletin of the American Meteorological Society*, 97(12), 2263–2273.